

The impact of simultaneous infections on phage-host ecology

Jaye Sudweeks^{1,a,b} and Christoph Hauert^{a,b}

¹Corresponding author. email: sudweeks@math.ubc.ca; postal address: 1984 Mathematics Rd, Vancouver, BC, V6T 1Z2, Canada

^aDepartment of Mathematics, University of British Columbia, 1984 Mathematics Road, Vancouver B.C. Canada, V6T 1Z2

^bDepartment of Zoology, University of British Columbia, 6270 University Boulevard, Vancouver B.C. Canada, V6T 1Z4

Phages use bacterial host resources to replicate, intrinsically linking phage and host survival. To understand phage dynamics, it is essential to understand phage-host ecology. A key step in this ecology is infection of bacterial hosts. Previous work has explored single and multiple, sequential infections. Here we focus on the theory of simultaneous infections, where multiple phages simultaneously attach to and infect one bacterial host cell. Simultaneous infections are a relevant infection dynamic to consider, especially at high phage densities when many phages attach to a single host cell in a short time window. For high bacterial growth rates, simultaneous infection can result in bi-stability: depending on initial conditions phages go extinct or co-exist with hosts, either at stable densities or through periodic oscillations of a stable limit cycle. This bears important consequences for phage applications such as phage therapy: phages can *persist* even though they cannot *invade*. Consequently, through spikes in phage densities it is possible to infect a bacterial population even when the phage basic reproductive number is less than one. In the regime of stable limit cycles, if timed right, only small densities of phage may be necessary.

population dynamics | bi-stability | bifurcations | limit cycles

1 Introduction

Viruses are parasites that inject their genetic material into a host cell and hijack the host's genetic apparatus to produce copies of themselves. In particular, phages are viruses that infect bacteria. Phages are ubiquitous in nature (Wasik and Turner, 2013) and have a widespread impact: for example, phages increase bacterial diversity (Abedon, 2008b) through (*i*) phage mediated predation: bacteria that are better competitors for resources tend

to have weaker defences against phages, thus phages help to level the playing field (Thingstad and Lignell, 1997); (ii) transduction: host DNA is (accidentally) packaged by the virus and transferred to other host bacteria (Day and Miller, 2008); (iii) lysogenic conversion: phage DNA is integrated into the host DNA and results in changes of the host phenotype (Abedon, 2008a; Barksdale and Arden, 1974). Phages also disrupt nutrient cycling in aquatic ecosystems, where phage induced lysis (i.e. killing the host cell by rupturing the cell wall) renders organic carbon unavailable to higher trophic levels (Wilhelm and Suttle, 1999). In addition, phages serve as a useful model system for testing ecological theory (Dennehy, 2012; Jessup et al., 2004; Kerr et al., 2008). Finally, phages have a frankly astonishing number of potential applications (García-Cruz et al., 2023). In the face of rising antibiotic resistant bacterial infections, perhaps the most well known application of phages is as an alternative antibiotic (Kortright et al., 2019). However, others have proposed the use of phages to decrease bacterial antibiotic resistance and virulence (Chan et al., 2016; Gordillo Altamirano et al., 2021; León and Bastías, 2015), treat dysbiosis (an imbalance in the gut microbial community that is associated with disease) (García-Cruz et al., 2023), and even combat non-bacterial diseases (Krishnan et al., 2014). Further proposed applications for phages include industrial uses as food preservatives (Endersen and Coffey, 2020), self replicating disinfectants (Song et al., 2021) and biofilm inhibitors (because bacteria within biofilms are often resistant to chemical disinfectants (Liu et al., 2022)), as well as use in pest control (Tikhe and Dimopoulos, 2022) and even as a tool to combat global warming (Boadi et al., 2004).

During the lytic infection cycle, phages use host machinery to replicate. After new phage particles are produced, the host cell is lysed (ruptured) to release phage replicates back into the environment. Crucially, because phages replicate using host cell resources they are dependent on their bacterial hosts to reproduce, and consequently the survival of a phage population is intimately tied to the survival of its host population. Thus in order to understand phages we must understand them in the context of their hosts, and ecological interactions between phages and their hosts are critical.

Phages infect host cells by adsorbing (attaching) to receptors on the host cell wall and then delivering the genomic content into the host cytoplasm. Phages are much smaller than bacteria and each host cell presents multiple receptors that phages can bind to, so multiple phages can adsorb to a single host cell, though not all adsorptions necessarily lead to infection. Multiple adsorptions become increasingly likely at higher phage densities (Christen et al., 1990; Turner and Duffy, 2008) and can become the dominant transmission mode at sufficiently high densities (Turner and Chao, 1999). If phage densities are very high, it is possible that multiple phages simultaneously adsorb to and then infect the same host cell. Here, we explore the impact of simultaneous infections on phage-host ecology. We define simultaneous infection as infections that occur within a very small time window and distinguish between simultaneous infection and previously studied forms of co-infection, where after a pause an already infected host cell is infected again. Interestingly, given sufficient time phages can prevent multiple, *sequential* infections through host cell manipulations (Joseph et al., 2009)

but these mechanisms are not applicable to the small time window relevant for simultaneous infections.

To demonstrate the relevance of simultaneous infections consider phage therapy, or the use of phages as an antibiotic. The basic premise of phage therapy is to use phages to lyse target bacterial populations (Kortright et al., 2019). In order for a bacterial population to be eliminated, all bacteria must be infected by at least one phage. However, due to the stochastic nature of phage adsorption, in order for all bacteria to be infected at least once high densities of phage must be added, and many bacteria will be adsorbed to multiple times (Abedon, 2016). Further, for both efficacy and in the interest of circumventing evolutionary arms races between phages and hosts (Hampton et al., 2020), it is preferable for adsorption and infection to happen quickly relative to the handling time of the sample and bacterial replication times (Goodridge, 2008). This creates a potential scenario where many adsorption events happen over a short time window, and it seems likely that simultaneous infection events would occur.

Take as another example the use of phages for biodetection, or to detect their bacterial hosts (Goodridge, 2008). Detection can be accomplished through several methods, for example by engineering phages to carry a reporter gene, labeling phages with fluorescent dye, or monitoring for phage amplification (or an increase in phage density which indicates replication has occurred), but in all cases the detection works only if phages adsorb to target bacteria. Beyond choosing phages that are well suited for the target bacteria, adding high density of phage is a reliable way to ensure adsorption. Adding an excess of phage has the added benefit of decreasing the adsorption time. As before, this would result in many adsorptions happening in a small time window, hence increasing the likelihood of simultaneous infections.

In both the phage therapy and biodetection examples, the crucial requirements are that bacteria are the limiting agent and that adsorption happens quickly (Goodridge, 2008). Both can be accomplished by high phage densities, creating potential scenarios where many adsorption events occur in a small time window and opening the door for simultaneous infections. Further, because phages can outnumber bacteria by an order of magnitude in many environments (Wasik and Turner, 2013), simultaneous infections may well be relevant in natural settings as well. If phages are concentrated around their bacterial hosts, say after a lysing event, then many adsorptions could occur in a short time frame, again creating the potential for simultaneous infections.

Here, we explore the dynamical impact of simultaneous infections on phage-host ecology. The interactions between phages and their hosts can be viewed from an ecological perspective as a predator-prey system with phages preying on bacteria, or from an epidemiological perspective with phages spreading through the bacterial population. Both perspectives provide helpful intuition and references for phage-host dynamics. In particular, for predator-prey systems we can rely on classical dynamical systems analysis, while from epidemiology we know the phages can invade when the phage basic reproductive number, R_0 , the expected number of new phages produced by a given phage at the initial spread of infection, exceeds one (Nowak and Bangham, 1996). Previous work in mathematical ecology has untangled some of the interwoven dynamics of phages and hosts

with and without co-infection (Alizon, 2013; Beretta and Kuang, 1998; Levin et al., 1977). Here we focus on the changes in the population dynamics arising from multiple, simultaneous infections of hosts. We use the well studied RNA phage φ_6 (Turner and Chao, 1999) as both reference and inspiration for the model we develop and analyze.

2 Model

(section:Model)

In the absence of phages, uninfected bacteria, H_U , divide at rate b_U , perish at rate d_U , and compete for resources at rate ξ . This results in classical logistic growth dynamics with a net per-capita growth rate of $r = b_U - d_U$, which admits two equilibria: the trivial equilibrium $H_0^* = 0$ and carrying capacity $H_U^* = r/\xi$.

Free living phages, P , can infect hosts. Single phages infect uninfected hosts at rate μ_1 while two phages simultaneously infect an uninfected host at rate μ_2 . An alternative derivation of our model that considers only sequential infections and assumes that a second infection can only occur in a small time window after the first infection is shown in appendix S2. Empirical work finds that infections are limited to few φ_6 phages per cell (Turner et al., 1999). We set the limit to coinfection at two phages per host cell for mathematical convenience. Besides, very high phage densities are required for simultaneous triple infections and beyond to significantly affect the dynamics.

After infection, phages replicate inside the host cell. Once the phage particle count inside the host cell has reached a threshold, say λ on average, the host lyses and releases phages back into the environment. We assume that lysing occurs once host resources are exhausted, and that the replication rate of phages is high, so the lysis time and final count of phage particles released is independent of whether one or two phages infected the host cell; accordingly, both single and simultaneous infection events result in an infected host, H_I .

Note that single infection events happen at rate $\mu_1 P$ while double infections happen at rate $\mu_2 P^2$. Consequently it seems natural that each infection in a double infection event occurs at rate $\mu_1 P$, and hence $\mu_2 P^2 = (\mu_1 P)^2$ such that $\mu_2 = \mu_1^2$. In theory this allows us to eliminate one parameter by setting $\mu_1 = \mu$ and $\mu_2 = \mu^2$, but keeping the rates separate provides further insights into interesting dynamical details.

We assume that infected hosts become passive in the sense that they are no longer able to reproduce or compete for resources with other hosts and perish generally at a faster rate than their uninfected counterparts, $d > d_U$. We also assume that phage densities are sufficiently higher than bacteria such that impacts of infection events on the phage pool can be neglected, see appendix S3. The rate at which infected hosts lyse is d , while phages degrade at the rate $d\kappa$. Hence, for $\kappa > 1$ phages are shorter lived than infected hosts, while for $\kappa < 1$ phages outlive infected hosts.

The events described above result in the following system of dynamical equations for the densities of

uninfected hosts, H_U , infected hosts H_I and free phage particles, P :

{eq:modelEqs}

$$\dot{H}_U = r H_U - \xi H_U^2 - \mu_1 H_U P - \mu_2 H_U P^2 \quad [1a] \quad \text{{eq:dotHu}}$$

$$\dot{H}_I = \mu_1 H_U P + \mu_2 H_U P^2 - d H_I \quad [1b] \quad \text{{eq:dotHi}}$$

$$\dot{P} = d \lambda H_I - d \kappa P. \quad [1c] \quad \text{{eq:dotP}}$$

See appendix S1 for a more detailed model derivation.

3 Results

{section:AnalysisNumerics}

In order to understand the ecological dynamics of Eq. (1), we first derive the equilibria and their stabilities to characterize the long term dynamics, followed by a bifurcation analysis to capture the distinct dynamical regimes. We use the burst size λ as a natural choice for the bifurcation parameter because it directly impacts the rate of phage production and hence their density. Standard analytical tools are used, when feasible, and complemented by numerical investigations.

3.1 Equilibria

All equilibria are written in the form $E_i = (H_U^*, H_I^*, P^*)$, and labeled by the index i , where H_U^* refers to the corresponding equilibrium density of uninfected hosts, H_I^* to that of infected hosts and P^* to the density of phages at this equilibrium. All three components of any biologically relevant equilibrium must be non-negative.

Two equilibria we have encountered already: the trivial equilibrium $E_0 = (0, 0, 0)$, which marks extinction of both hosts and phages, as well as the uninfected equilibrium $E_U = (\frac{r}{\xi}, 0, 0)$, which applies in the absence of phages or upon their extinction.

For suitable parameters interior equilibria may exist. From Eq. (1c) it follows that

$$P^* = \frac{\lambda}{\kappa} H_I^* \quad [2] \quad \text{{eq:Pstar}}$$

must hold at any equilibrium. Similarly, a relation between H_U^* and H_I^* can be derived from Eq. (1a). Using Eq. (2) and after eliminating the trivial solution (dividing by H_U^*), we find

$$H_U^* = -\frac{\lambda^2 \mu_2}{\kappa^2 \xi} H_I^{*2} - \frac{\lambda \mu_1}{\kappa \xi} H_I^* + \frac{r}{\xi} \quad [3] \quad \text{{eq:HuStar}}$$

Equipped with Eqs. (2), (3) we can express Eq. (1b) at any interior equilibrium solely in terms of H_I^* . After eliminating the trivial solution as well as common constant factors, we obtain the equilibrium densities of

infected hosts, H_I^* , as implicit solutions given by the roots of the cubic polynomial

$$f(H_I) = \lambda^4 \mu_2^2 H_I^3 + 2\kappa \lambda^3 \mu_1 \mu_2 H_I^2 + \lambda^2 \kappa^2 (\mu_1^2 - \mu_2 r) H_I - \kappa^3 \lambda \mu_1 r + d \kappa^4 \xi. \quad [4] \quad \text{(eq:cubicHi)}$$

Each root, H_I^* , refers to one of up to three interior equilibria, though none may be biologically relevant. Unfortunately the roots of cubic polynomials yield unwieldy expressions but fortunately based on the discriminant and Descartes' rule of signs, we can still analytically determine the number of biologically relevant H_I^* , see appendix S5. In summary, we obtain two dynamical scenarios based on the rate of reproduction of uninfected hosts, r . Each scenario results in up to two equilibrium densities of infected host cells with $H_I^* > 0$:

A. low bacterial growth rates, no bi-stability: $r \leq \mu_1^2/\mu_2$

- (i) $\lambda < \lambda_T$: no interior equilibrium,
- (ii) $\lambda > \lambda_T$: a single interior equilibrium;

B. high bacterial growth rates, bi-stability possible: $r > \mu_1^2/\mu_2$

- (i) $\lambda < \lambda_S$: no interior equilibrium,
- (ii) $\lambda_S < \lambda < \lambda_T$: two interior equilibria,
- (iii) $\lambda > \lambda_T$: a single interior equilibrium.

with $\lambda_T = d\kappa\xi/(r\mu_1)$ and $\lambda_S = -d\xi\kappa(2\mu_1^3 + 9\mu_1\mu_2r - 2(\mu_1^2 + 3\mu_2r)^{3/2})/(\mu_2r^2(\mu_1^2 + 4\mu_2r))$, see appendix S5. Note that the biological relevance of a given H_I^* does not inherently imply that the corresponding interior equilibrium E_i is biologically relevant, too. While from Eq. (2) we know that the sign of P^* is the same as that of H_I^* , in contrast from Eq. (3) we see that, in principle, the uninfected component, H_U^* , of an interior equilibrium can become negative for sufficiently large infected densities, $H_I^* > \kappa(-\mu_1 + \sqrt{\mu_1^2 + 4\mu_2r})/(2\mu_2\lambda)$. However, in appendix S6 we show that H_I^* has an upper bound below that threshold and hence whenever H_I^* is biologically relevant H_U^* and P^* are as well.

3.2 Stability

It is immediately clear that the trivial, extinction equilibrium, E_0 , is always unstable for $r > 0$ because $\dot{H}_U > 0$ for small P , see Eq. (1a). Similarly, the uninfected equilibrium, E_U , is stable for $\lambda < \lambda_T = d\kappa\xi/(r\mu_1)$, which is easily confirmed by checking the eigenvalues of the Jacobian at the equilibrium, see appendix S4.

A complementary and more intuitive approach to arrive at the same conclusion is to consider the basic reproductive number, R_0 , of phages: the per capita rate of infection is μ_1 and phages have an expected lifespan of $1/(d\kappa)$. Thus, a phage introduced into an entirely uninfected host cell population at its equilibrium, E_U with

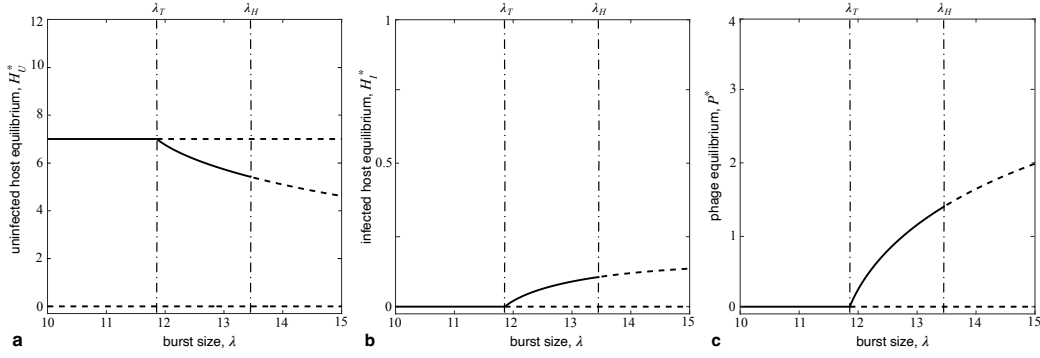


Fig. 1. Bifurcation diagram for the dynamics in Eq. (4) with $r < \mu_1^2/\mu_2$ as a function of the burst size λ . Each panel depicts one component of the stable (solid lines) and unstable (dashed lines) equilibria, $E_i = (H_U^*, H_I^*, P^*)$: **a** uninfected hosts, H_U^* , **b** infected hosts, H_I^* , and **c** phage densities, P^* . The trivial, extinction equilibrium, E_0 , is always unstable and the uninfected equilibrium E_U is stable for small λ . There are two bifurcations (dash-dotted vertical lines): a transcritical bifurcation at $\lambda_T = d\kappa\xi/(r\mu_1) \approx 11.86$, where a stable interior equilibrium appears and E_U turns unstable, followed by a Hopf-bifurcation at $\lambda_H \approx 13.57$ where the interior equilibrium loses stability. This results in three dynamical regimes: for $\lambda < \lambda_T$ the uninfected equilibrium, E_U , is stable and a global attractor; for $\lambda_T < \lambda < \lambda_H$ the interior equilibrium, E_I , is a global attractor; and finally for $\lambda > \lambda_H$ all equilibria are unstable and stable limit cycles develop. Parameters: $r = 0.7$, $\xi = 0.1$, $\mu_1 = 0.1$, $\mu_2 = 0.01$, $d = 8.3$, $\kappa = 1$.

{fig:r11}

$H_U^* = r/\xi$, infects $r\mu_1/(d\kappa\xi)$ cells on average. Note that double infections are negligible because initial phage densities are small. The expected lifespan of an infected host cell is $1/d$ and produces phages at the rate $d\lambda$. Overall, initially each phage produces $R_0 = r\mu_1\lambda/(d\kappa\xi)$ new phages and phages can invade if $R_0 > 1$, or equivalently if $\lambda > \lambda_T$, where λ_T the threshold for E_U to become unstable.

Calculating the stability of the interior equilibria, E_i , using the Jacobian is analytically intractable. Instead we turn to numerical analysis for an illustrative set of parameters. For more details on parameters see appendix S8.

3.3 Bifurcations

{subsection:bifurcations}

The number and stability of all equilibria, except the trivial extinction equilibrium, change when varying the burst size λ , the expected number of phages produced by each infected host bacterium. Hence, λ presents itself as an ideal and biologically relevant choice for a bifurcation parameter.

Let us first focus on the simpler case with $r < \mu_1^2/\mu_2$, see Fig. 1. For small λ the uninfected equilibrium E_U is stable. At λ_T a stable interior equilibrium E_I appears through a transcritical bifurcation and the uninfected equilibrium E_U loses stability. Further increases in λ result in E_I losing stability through a Hopf-bifurcation at λ_H , which is unfortunately analytically inaccessible. This yields three dynamical regimes illustrated through phase plane projections in Fig. 2.

- (i) $\lambda < \lambda_T$: only the uninfected equilibrium, E_U , is stable. All trajectories are drawn to E_U , which means the phages invariably go extinct regardless of their initial density, see Fig. 2 a, d.
- (ii) $\lambda_T < \lambda < \lambda_H$: only the interior equilibrium, E_I , is stable. All trajectories are drawn to E_I , such that

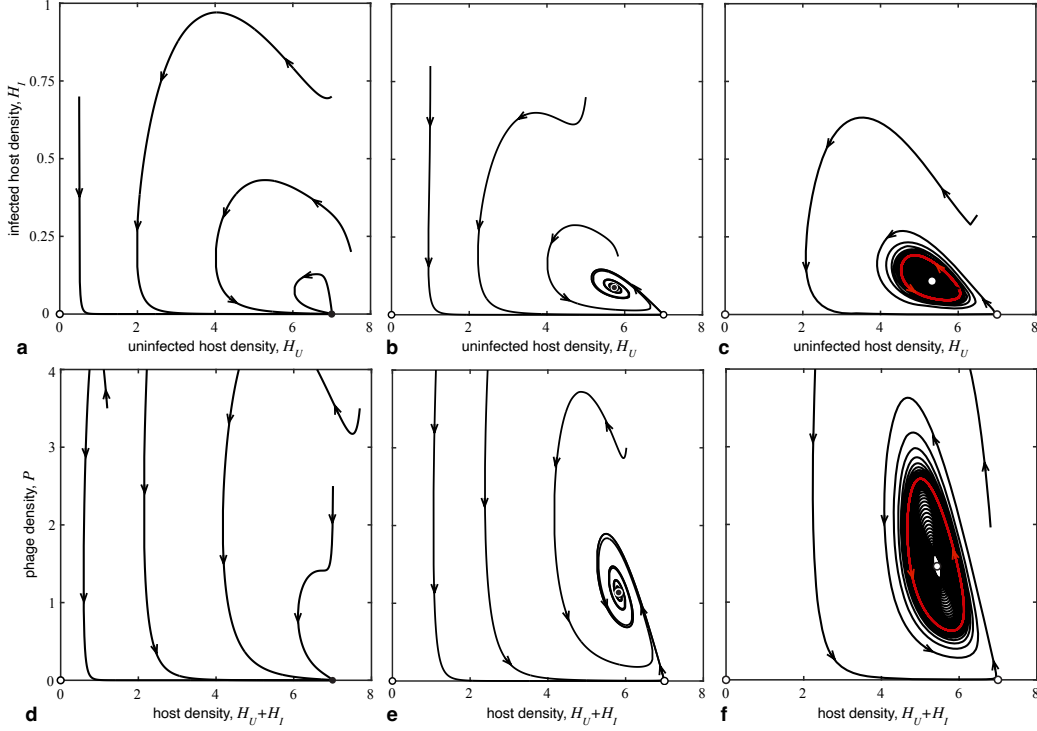


Fig. 2. Projections of the phase space depicting the characteristics of the three dynamical regions for $r < \mu_1^2/\mu_2$. The top row shows infected, H_I , versus uninfected, H_U , host densities and the bottom row shows phage densities, P , versus host densities, $H_U + H_I$. Note that trajectories may intersect because the panels show projections of a three dimensional phase space. Dots mark stable (filled) and unstable (open) equilibria. Stable limit cycles are shown in red. **a, d** $\lambda = 11$: all trajectories converge to E_U and phages go extinct. **b, e** $\lambda = 13$: E_U becomes unstable and the stable interior equilibrium E_I is a global attractor. **c, f** $\lambda = 13.6$: the interior equilibrium E_I becomes unstable and the attractor E_I is replaced by a stable limit cycle. Parameters: same as in Fig. 1.

(fig:ppr11)

host and phages stably co-exist. More specifically, because E_U is now unstable, phages are able to proliferate and invade the host population, see Fig. 2 b, e.

- (iii) $\lambda > \lambda_H$: no stable equilibrium remains. The Hopf-bifurcation together with the lack of other stable equilibria is a strong indicator of stable limit cycles, which has been confirmed numerically, see Fig. 2 c, f.

Recall that the per-capita rate for single infections is $\mu_1 P$ whereas for double infections it is $\mu_2 P^2$. Hence, double infections are the dominant mode if $P > \mu_1/\mu_2$ and single infections otherwise. In Fig. 1c the phage densities at equilibrium never reach the threshold for double infections to dominate. Thus in this case double infections play only a marginal role. Note that the non-generic case, $r = \mu_1^2/\mu_2$, is qualitatively the same as $r < \mu_1^2/\mu_2$.

The case with $r > \mu_1^2/\mu_2$ is more interesting because it results in richer dynamics, see Fig. 3. For small λ the uninfected equilibrium E_U is again stable. At λ_S a stable/unstable pair of interior equilibria, E_{I_s} and

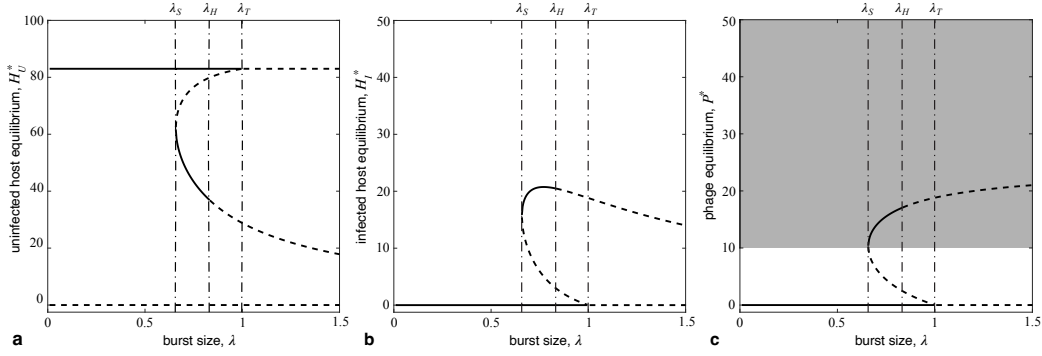


Fig. 3. Bifurcation diagram for the dynamics in Eq. (4) with $r > \mu_1^2/\mu_2$ as a function of the burst size λ . Each panel depicts one component of the stable (solid lines) and unstable (dashed lines) equilibria, $E_i = (H_U^*, H_I^*, P^*)$: **a** uninfected hosts, H_U^* , **b** infected hosts, H_I^* , and **c** phage densities, P^* , where the shaded area marks densities for which double infections dominate. The trivial equilibrium, E_0 , is always unstable and the uninfected equilibrium E_U is stable for small λ . There are three bifurcations (dash-dotted vertical lines): a saddle node bifurcation at $\lambda_S \approx 0.6585$ (c.f. λ_- in Eq. (S16)) where a pair (stable, E_{I^s} and unstable, E_{I^u}) of interior equilibria appear; a Hopf-bifurcation at $\lambda_H \approx 0.8329$ where E_{I^s} loses its stability; and finally a transcritical bifurcation at $\lambda_T = 1$ where the (originally) unstable interior equilibrium, E_{I^u} , disappears and E_U loses stability. This results in four dynamical regimes: for $\lambda < \lambda_S$ the uninfected equilibrium, E_U , is stable and a global attractor; for $\lambda_S < \lambda < \lambda_H$ the dynamics are bi-stable with attractors E_U and E_{I^s} ; for $\lambda_H < \lambda < \lambda_T$ the dynamics remain bi-stable but the attractor E_{I^s} is replaced by a stable limit cycle, see Fig. 4 c, g. Finally, for $\lambda > \lambda_T$ no stable equilibria exist but the stable limit cycle persists, see Fig. 4 d, h. Parameters: $r = 8.3$, $\xi = 0.1$, $\mu_1 = 0.1$, $\mu_2 = 0.01$, $d = 8.3$, $\kappa = 1$ (same as in Fig. 1 except for r).

(fig:r91)

E_{I^u} , respectively, appear through a saddle node bifurcation. Then, at λ_H , the stable interior equilibrium, E_{I^s} , loses stability through a Hopf-bifurcation, leaving E_U as the only stable equilibrium. Finally at λ_T the (originally) unstable interior equilibrium, E_{I^u} , disappears through a transcritical bifurcation with the uninfected equilibrium, E_U , which loses stability at the same time. At this point no stable equilibria remain and hence stable limit cycles are expected. Fig. 4 depicts illustrative phase plane projections for each of the four resulting dynamical regimes.

- (i) $\lambda < \lambda_S$: only the uninfected equilibrium, E_U , is stable. All trajectories are drawn to E_U , which means the phages invariably go extinct regardless of their initial density, Fig. 4 a, e.
- (ii) $\lambda_S < \lambda < \lambda_H$: a pair of interior equilibria appears but only one, E_{I^s} , is stable. This results in bi-stable dynamics with two basins of attraction. Depending on the initial conditions trajectories converge to either (a) E_U , which marks the extinction of the phage population, or (b) E_{I^s} , indicating stable co-existence of bacteria and phages, see Fig. 4 b, f.
- (iii) $\lambda_H < \lambda < \lambda_T$: both interior equilibria are now unstable and only E_U remains stable. However, this does not imply that E_U is globally stable. Instead, the bi-stability remains but E_{I^s} as an attractor is replaced by a stable limit cycle, see Fig. 4 c, g.
- (iv) $\lambda > \lambda_T$: no stable equilibrium remains. The limit cycle is now a global attractor, see Fig. 4 d, h.

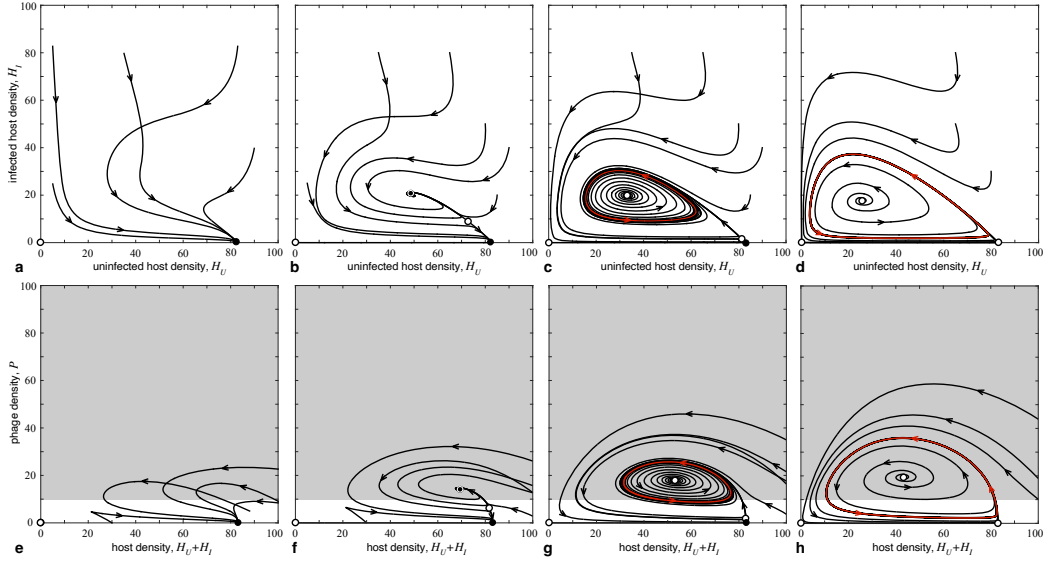


Fig. 4. Projections of the phase space depicting the characteristics of the four dynamical regions for $r > \mu_1^2/\mu_2$. The top row shows infected, H_I , versus uninfected, H_U , host densities and the bottom row shows phage densities, P , versus host densities, $H_U + H_I$. Shaded regions on the bottom row mark phage densities for which double infections dominate. Note that trajectories may cross because the panels show projections of a three dimensional phase space. Dots mark stable (filled) and unstable (open) equilibria. Stable limit cycles are shown in red. **a, e** $\lambda = 0.5$: all trajectories converge to E_U and phages go extinct. **b, f** $\lambda = 0.7$: a pair of interior equilibria appear, E_{I^u} and E_{I^s} , and the dynamics become bi-stable with attractors E_U and E_{I^s} . **c, g** $\lambda = 0.9$: the interior equilibrium E_{I^s} becomes unstable and the attractor E_{I^s} is replaced by a limit cycle. **d, h** $\lambda = 1.1$: the (originally) unstable interior equilibrium E_{I^u} disappears and only a globally stable limit cycle remains. Parameters: same as in Fig. 3.

(fig:prrg1)

The major difference between the dynamics of the two cases is the emergence of bi-stability for $\lambda_S < \lambda < \lambda_T$ in the case $r > \mu_1^2/\mu_2$. In Fig. 4 b, f, for $\lambda_S < \lambda < \lambda_H$ there are two basins of attraction, and some trajectories are drawn to the stable equilibrium E_{I^s} , indicating stable co-existence of phage and host. Similarly, in Fig. 4 c, g, for $\lambda_H < \lambda < \lambda_T$ trajectories are drawn into a stable limit cycle, indicating fluctuating co-existence of phage and host. Crucially, note that the phage basic reproductive number $R_0 < 1$ for all $\lambda_S < \lambda < \lambda_T$, meaning small densities of phage are not be able to invade and establish. However, due to bi-stability, sufficiently large densities of phage can persist and co-exist with hosts, which implies that a shock in phage densities would allow phages to get a foothold and persist.

When $r < \mu_1^2/\mu_2$ (no bi-stability) results are in agreement with previous work that considers only single infections (compare Fig. 2 with Figs. 1-3 of (Beretta and Kuang, 1998)). This suggests that Eq. (1) can be interpreted as a generalized model that encompasses this previous work while allowing investigation of the impact of simultaneous infections, see appendix S8 for more details. The contributions of double infections lead to a major shift in dynamics at the threshold $r = \mu_1^2/\mu_2$. The threshold can be written as $(rH_U)(P^2\mu_2H_U) = (\mu_1PH_U)^2$, which admits a more intuitive interpretation in terms of two types of simultaneous events: on the left hand side replication of an uninfected host and a double infection event, and

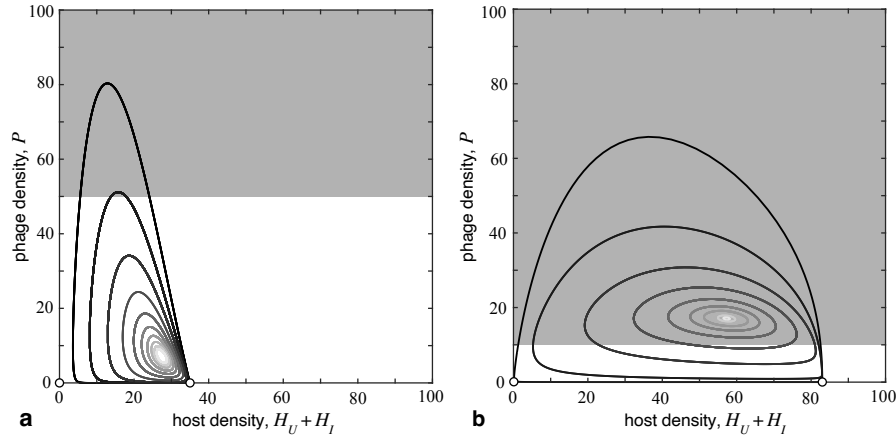


Fig. 5. Stable limit cycles for increasing λ : in **a** $r < \mu_1^2/\mu_2$ and $\lambda_H \approx 13.48$ while in **b** $r > \mu_1^2/\mu_2$ and $\lambda_H \approx 0.8328$. For $\lambda > \lambda_H$ a small limit cycle appears, which gradually grows with λ (light to dark shades of grey). The shaded area marks regions for which phage densities are sufficiently high such that double infections dominate. Along the horizontal axis the open circles mark the locations of the two unstable equilibria: extinction, E_0 , as well as the uninfected equilibrium, E_U . Note that the location of the interior equilibrium shifts with λ (not shown, c.f. Figs. 1, 3). Parameters: $\xi = 0.1, \mu_1 = 0.1, \mu_2 = 0.01, d = 8.3, \kappa = 1$ with **a** $r = 0.7, \lambda \in \{13.50, 13.51, 13.54, 13.59, 13.67, 13.80, 14.05, 14.47, 15.20, 16.48\}$, and **b** $r = 8.3, \lambda \in \{0.8331, 0.8335, 0.8345, 0.8368, 0.8427, 0.8577, 0.8954, 0.9901, 1.2298, 1.8329\}$.

{fig:cycles}

on the the right hand side two simultaneous single infection events. Hence, we can interpret our different dynamical regimes as a balance of these simultaneous events. If the rate at which a newly emerged uninfected host is doubly infected is higher than the rate at which simultaneously two separate uninfected hosts are singly infected, then bi-stability can occur for sufficiently high λ .

As previously noted, in Fig. 1 c the interior equilibrium, E_I , lies entirely in the region where single infections prevail. In fact, for $r < 2\mu_1/\mu_2$ single infections always dominate at E_I , see appendix S7. In contrast, in Fig. 3 c the (originally stable) interior equilibrium, E_{I^s} , lies in the shaded region where double infections dominate. In general, for $r > 2\mu_1^2/\mu_2$ double infections dominate at E_{I^s} for sufficiently large λ , see appendix S7. Note that the transition between the two dynamical cases (no bi-stability vs. bi-stability) does not align exactly with the transition away from dominant single infections at E_{I^s} , and there is a region $\mu_1^2/\mu_2 < r < 2\mu_1^2/\mu_2$ that exhibits bi-stability but single infections still dominate at E_{I^s} regardless of λ .

In both dynamical regimes, the size of the limit cycles for $\lambda > \lambda_H$ increases with λ , see Fig. 5. For larger λ , the limit cycles periodically alternate between the two domains of dominant single and double infections. In addition, as λ increases the limit cycles approach vanishing phage densities and get closer to both the extinction equilibrium, E_0 , as well as the uninfected equilibrium, E_U . As a consequence the dynamics become increasingly prone to stochastic effects, which can easily result in the extinction of the phage population or of both hosts and phages.

The parameter κ , which sets the relative lifespan of phages versus hosts and thus impacts the density of

phages in the environment and accordingly the rate of infections, has surprisingly little impact on the dynamics, see appendix S9.

4 Discussion

(section:Discussion)

Our model describes a phage-host system where multiple phages can simultaneously infect a single host. Considering the high densities of phage proposed for use in various applications, as well as the high densities of phage in many natural settings, simultaneous infections are a natural and relevant infection dynamic to consider. Our results shed light on several ecological features of this system and suggest interesting evolutionary implications.

4.1 Impact of net bacterial growth rate

We find that the qualitative dynamics depend on the net bacterial growth rate, r , compared to the ratio of the rates of single versus simultaneous double infections, μ_1^2/μ_2 . An intuitive assumption posits that if single infections occur at a rate proportional to $\mu_1 P$ then it is natural that double infections occur proportional to $(\mu_1 P)^2$, which sets the threshold between the two dynamical regimes to $r = 1$. Qualitatively different dynamics occur if the rate at which a newly emerged uninfected host is doubly infected is higher versus lower than the rate at which simultaneously two separate uninfected hosts are singly infected.

If bacterial growth rates are low ($r \leq \mu_1^2/\mu_2$), then $R_0 < 1$ is sufficient to eliminate phage infection, see Fig. 1, and the resulting dynamics are in excellent agreement with a previous study that models only single infection (Beretta and Kuang, 1998). Fittingly, in our model single infections always occur at a higher rate than double infections for low bacterial growth rates. Accordingly, our model can be interpreted as a generalized model that encompasses this previous work while further allowing for the investigation of dynamical features arising through simultaneous infections. Indeed, for high bacterial growth rates ($r > \mu_1^2/\mu_2$) dynamics are bi-stable and $R_0 < 1$ is necessary but not sufficient for phage elimination. Bi-stability has important ramifications for both phage applications and disease management, which are discussed in full detail below. Interestingly, our results are in line with previous work on cooperative hunting in predator-prey systems, which similarly found that bi-stability in the predator population is only possible for sufficiently high prey growth rates (Alves and Hilker, 2017).

The parameter κ sets the relative life spans of hosts versus phages and thus influences the environmental density of phages. When bacterial growth rates are low ($r < \mu_1^2/\mu_2$), the dynamics are qualitatively identical regardless of κ . In contrast, when bacterial growth rates are high ($r > \mu_1^2/\mu_2$) the relative lifespans matter: if infected hosts outlive phages, ($\kappa \geq 1$) again no qualitative changes. However, if phages degrade more slowly than infected hosts lyse ($\kappa < 1$), the dynamics admit a region where the infected equilibrium E_{I^s} is a global attractor. Thus, for a range of burst sizes, λ , phages can invade and reach a stable density. Otherwise such

dynamics are only observed for low bacterial growth rates.

4.2 Limit cycles, extinction risk, and evolutionary implications

Phage-host dynamics often exhibit limit cycles, as is typical of predator-prey relationships. Specifically, in our model large λ invariably result in stable limit cycles regardless of the host growth rate r : if uninfected hosts abound, phages always succeed in infecting a host but then large burst sizes result in a rapid increase in phage density, and phages quickly spread through the host population. As a consequence, the density of uninfected, susceptible hosts declines and phage replication slows down. The resulting decline of phage densities allows the hosts to recover and the cycle restarts. Experimental work with phages often requires controlling the relative density of phages and hosts, for example to control the expected number of bacteria that are infected by multiple phages (Turner and Chao, 1999, 2003). Thus, even though controlling phage density in experiments may be inevitable, it may also obscure important ecological dynamics.

Further, the size of the stable limit cycles increase with λ such that trajectories periodically get arbitrarily close not only to vanishing phage densities but also to the extinction equilibrium, see Fig. 5. In populations with small numbers stochastic effects matter (Huang et al., 2015; Traulsen et al., 2012), and the smallest perturbation could easily result in the extinction of phages, or both phages and their host. In cases where phages drive the host population extinct they inevitably follow suit because they have exhausted their resource for replication. Thus while increasing the burst size λ increases $R_0 = r\mu_1\lambda/(d\kappa\xi)$ and hence makes it easier for phages to invade, larger λ counter-intuitively also carry the inherent risk of extinction of phages or even both populations.

Our work focuses on the *ecological* impact of simultaneous infections but suggests an interesting *evolutionary* question. In our model, host death is inevitable after infection. However, the burst size λ influences phage density and accordingly the rate at which hosts are infected and then lyse. Consequently λ makes a suitable proxy for virulence, or the increase in host mortality due to infection, as noted in the discussion of Dennehy and Turner (2004). Though λ is a key parameter in our analysis, it does not evolve.

A natural expectation is that larger burst sizes would benefit the phage population. However, our analysis suggests that thereby phages also deplete their resources for further replication. Still, since selection acts first and foremost on the level of individuals, traits which produce more offspring should generally increase in frequency. This suggests tensions between selective pressures on individual phages and the viability of the phage population overall. In extreme cases this mismatch in individual fitness and population viability can lead to *evolutionary suicide*, where viable populations adapt in a way that they can no longer persist (Ferriere and Legendre, 2013; Parvinen, 2005). Conversely, because of the interplay between evolutionary and ecological processes (such as fluctuation in host densities), parasites should evolve toward decreased virulence (Lenski and May, 1994). Moreover, co-infection of hosts (singly infected cells remain susceptible and can be infected again) (Alizon, 2013) can result in feedback loops between the rate at which susceptible individuals acquire

a disease (the force of infection) and virulence: when double infections are common increased virulence is favored; however, increased pathogen virulence decreases the force of infection, favoring decreased virulence once more (van Baalen and Sabelis, 1995).

4.3 Disease management and phage applications

When bacterial growth rates are high ($r > \mu_1^2/\mu_2$) simultaneous double infections result in bi-stabilities between the uninfected equilibrium, E_U , and stable co-existence of phages and hosts either at an interior equilibrium, E_{I^s} , or through periodic oscillations of a stable limit cycle. In particular, the bi-stability enables phages to *persist* even though they are not able to *invade* because their basic reproductive number R_0 is less than 1, see Fig. 3. This implies that a shock in phage densities would allow phages to get a foothold and persist.

Bi-stabilities have important ramifications for disease management (Dushoff et al., 1998). When bacterial growth rates are higher ($r > \mu_1^2/\mu_2$), ensuring $R_0 < 1$ is necessary but not sufficient to eliminate phages, see Fig. 3. Instead, it is required to either lower R_0 to a much greater extent, or to manipulate the ecology by introducing measures to lower phage densities through other means, which could make eliminating a problematic phage population difficult. However, it is enough to apply control measures just once to eliminate phages. Further, in the case of stable limit cycles, if timed right, a very small intervention may be sufficient to push the dynamics into the other basin of attraction, see Fig. 2 & 4. In other words, there is the opportunity eliminate a detrimental strain with limited effort.

For high bacterial growth rates ($r > \mu_1^2/\mu_2$), in the region of bi-stability sufficiently densities of phages can persist even when they cannot invade. In the context of phage applications, introducing high densities of phage to a target bacterial population should be enough to ensure that the phage population takes off, even if the phage would not be able to establish from very low densities. Indeed, in the region of limit cycles, the necessary shock of phage density may be relatively low, implying that it may be possible to introduce a desired phage strain with limited effort.

5 Acknowledgements

We thank Alun Lloyd and Laura Parfrey for helpful discussion on an earlier version of the manuscript, as well as Arne Traulsen and Gabriel Currier for insightful comments. The authors acknowledge funding by the Natural Science and Engineering Research Council of Canada, Discovery Grant RGPIN-2021-02608 to C.H.

6 Declaration of interest

Declarations of interest: none

References

- S. T. Abedon. Phages, ecology, evolution. [Abedon \(2008b\)](#), pages 1–28. .
- S. T. Abedon, editor. *Bacteriophage ecology: population growth, evolution, and impact of bacterial viruses*. Cambridge University Press, 2008b. .
- S. T. Abedon. Phage therapy dosing: The problem (s) with multiplicity of infection (moi). *Bacteriophage*, 6: e1220348, 2016.
- S. Alizon. Co-infection and super-infection models in evolutionary epidemiology. *Interface Focus*, 3(6): 20130031, 2013.
- M. T. Alves and F. M. Hilker. Hunting cooperation and allee effects in predators. *Journal of theoretical biology*, 419:13–22, 2017.
- L. Barksdale and S. B. Arden. Persisting bacteriophage infections, lysogeny, and phage conversions. *Annual Reviews in Microbiology*, 28:265–300, 1974.
- E. Beretta and Y. Kuang. Modeling and analysis of a marine bacteriophage infection. *Mathematical Biosciences*, 149(1):57–76, 1998.
- D. Boadi, C. Benchaar, J. Chiquette, and D. Massé. Mitigation strategies to reduce enteric methane emissions from dairy cows: Update review. *Canadian Journal of Animal Science*, 84:319–335, 2004.
- B. K. Chan, M. Sistro, J. E. Wertz, K. E. Kortright, D. Narayan, and P. E. Turner. Phage selection restores antibiotic sensitivity in *mdr pseudomonas aeruginosa*. *Scientific reports*, 6:26717, 2016.
- L. Christen, J. Seto, and E. G. Niles. Superinfection exclusion of vaccinia virus in virus-infected cell cultures. *Virology*, 174(1):35–42, 1990.
- M. J. Day and R. V. Miller. Phage ecology of terrestrial environments. In [Abedon \(2008b\)](#), pages 281–301. .
- J. J. Dennehy. What can phages tell us about host-pathogen coevolution? *Journal of Evolutionary Biology*, 2012:396165, 2012. .
- J. J. Dennehy and P. E. Turner. Reduced fecundity is the cost of cheating in rna virus φ 6. *Proceedings of the Royal Society of London. Series B: Biological Sciences*, 271(1554):2275–2282, 2004.
- J. Dushoff, W. Huang, and C. Castillo-Chavez. Backwards bifurcations and catastrophe in simple models of fatal diseases. *Journal of Mathematical Biology*, 36:227–248, 1998.
- L. Endersen and A. Coffey. The use of bacteriophages for food safety. *Current Opinion in Food Science*, 36: 1–8, 2020.
- R. Ferriere and S. Legendre. Eco-evolutionary feedbacks, adaptive dynamics and evolutionary rescue theory. *Philosophical Transactions of the Royal Society B*, 368(1610):20120081, Jan. 2013. ISSN 0962-8436, 1471-2970. .
- J. C. García-Cruz, D. Huelgas-Méndez, J. S. Jiménez-Zúñiga, X. Rebollar-Juárez, M. Hernández-Garnica,

- A. M. Fernández-Presas, F. M. Husain, R. Alenazy, M. Alqasmi, T. Albalawi, et al. Myriad applications of bacteriophages beyond phage therapy. *PeerJ*, 11:e15272, 2023.
- L. D. Goodridge. Phages, bacteria, and food. In [Abedon \(2008b\)](#), pages 302–331. .
- F. Gordillo Altamirano, J. H. Forsyth, R. Patwa, X. Kostoulias, M. Trim, D. Subedi, S. K. Archer, F. C. Morris, C. Oliveira, L. Kielty, et al. Bacteriophage-resistant acinetobacter baumannii are resensitized to antimicrobials. *Nature microbiology*, 6:157–161, 2021.
- H. G. Hampton, B. N. Watson, and P. C. Fineran. The arms race between bacteria and their phage foes. *Nature*, 577:327–336, 2020.
- W. Huang, C. Hauert, and A. Traulsen. Stochastic game dynamics under demographic fluctuations. *Proceedings of the National Academy of Sciences*, 112(29):9064–9069, Jul 2015. .
- C. M. Jessup, R. Kassen, S. E. Forde, B. Kerr, A. Buckling, P. B. Rainey, and B. J. Bohannan. Big questions, small worlds: microbial model systems in ecology. *Trends in Ecology & Evolution*, 2004.
- S. B. Joseph, K. A. Hanley, L. Chao, and C. L. Burch. Coinfection rates in $\phi 6$ bacteriophage are enhanced by virus-induced changes in host cells. *Evolutionary Applications*, 2(1):24–31, 2009. .
- B. Kerr, J. West, and B. J. M. Bohannan. Bacteriophages: models for exploring basic principles of ecology. In [Abedon \(2008b\)](#), pages 31–63. .
- K. E. Kortright, B. K. Chan, J. L. Koff, and P. E. Turner. Phage therapy: a renewed approach to combat antibiotic-resistant bacteria. *Cell Host & Microbe*, 25(2):219–232, 2019.
- R. Krishnan, H. Tsubery, M. Y. Proschitsky, E. Asp, M. Lulu, S. Gilead, M. Gartner, J. P. Waltho, P. J. Davis, A. M. Hounslow, et al. A bacteriophage capsid protein provides a general amyloid interaction motif (gaim) that binds and remodels misfolded protein assemblies. *Journal of molecular biology*, 426:2500–2519, 2014.
- R. E. Lenski and R. M. May. The evolution of virulence in parasites and pathogens: Reconciliation between two competing hypotheses. *Journal of Theoretical Biology*, 169:253–265, Aug 1994.
- M. León and R. Bastías. Virulence reduction in bacteriophage resistant bacteria. *Frontiers in microbiology*, 6:343, 2015.
- B. R. Levin, F. M. Stewart, and L. Chao. Resource-limited growth, competition, and predation: a model and experimental studies with bacteria and bacteriophage. *The American Naturalist*, 111(977):3–24, 1977.
- S. Liu, H. Lu, S. Zhang, Y. Shi, and Q. Chen. Phages against pathogenic bacterial biofilms and biofilm-based infections: a review. *Pharmaceutics*, 14:427, 2022.
- M. A. Nowak and C. R. Bangham. Population dynamics of immune responses to persistent viruses. *Science*, 272(5258):74–79, 1996.
- K. Parvinen. Evolutionary suicide. *Acta Biotheoretica*, 53(3):241–264, 2005.
- J. Song, H. Ruan, L. Chen, Y. Jin, J. Zheng, R. Wu, and D. Sun. Potential of bacteriophages as disinfectants to control of staphylococcus aureus biofilms. *BMC microbiology*, 21:1–14, 2021.

- T. F. Thingstad and R. Lignell. Theoretical models for the control of bacterial growth rate, abundance, diversity and carbon demand. *Aquatic Microbial Ecology*, 13:19–27, 1997.
- C. V. Tikhe and G. Dimopoulos. Phage therapy for mosquito larval control: a proof-of-principle study. *Mbio*, 13:e03017–22, 2022.
- A. Traulsen, J. C. Claussen, and C. Hauert. Stochastic differential equations for evolutionary dynamics with demographic noise and mutations. *Physical Review E*, 85:041901, 2012.
- P. E. Turner and L. Chao. Prisoner’s dilemma in an RNA virus. *Nature*, 398:441–443, 1999.
- P. E. Turner and L. Chao. Escape from prisoner’s dilemma in RNA phage $\phi 6$. *The American Naturalist*, 161(3): 497–505, Mar 2003.
- P. E. Turner and S. Duffy. Evolutionary ecology of multiple phage adsorption and infection. In [Abedon \(2008b\)](#), pages 195–216. .
- P. E. Turner, C. L. Burch, K. A. Hanley, and L. Chao. Hybrid frequencies confirm limit to coinfection in the rna bacteriophage $\phi 6$. *Journal of virology*, 73:2420–2424, 1999.
- M. van Baalen and M. W. Sabelis. The dynamics of multiple infection and the evolution of virulence. *The American Naturalist*, 146(6):881–910, 1995.
- B. R. Wasik and P. E. Turner. On the biological success of viruses. *Annual Review of Microbiology*, 67:519–541, 2013.
- S. W. Wilhelm and C. A. Suttle. Viruses and nutrient cycles in the sea: viruses play critical roles in the structure and function of aquatic food webs. *Bioscience*, 49:781–788, 1999.

Supplementary Material for The Impact of Simultaneous Infections on Phage-Host Ecology

Jaye Sudweeks & Christoph Hauert

S1 Full model derivation

In order to build our model, we consider microscopic reaction processes between phages and their bacterial hosts. First, in the absence of phages, the uninfected bacteria, H_U , divide at a rate b_U , perish at a rate d_U and compete for resources with other hosts at rate ξ . The subscript U refers to the fact that the hosts under consideration are uninfected. In terms of reaction kinetics this yields the following three equations:



Based on the mass-action principle, this results in classical logistic growth dynamics for uninfected hosts:

$$\dot{H}_U = r H_U - \xi H_U^2, \quad [\text{S2}]$$

where $r = b_U - d_U$ denotes the net per capita rate of growth. Naturally, Eq. (S2) admits two equilibria, the trivial equilibrium $H_0^* = 0$ and carrying capacity $H_U^* = r/\xi$. For $r < 0$ the trivial equilibrium H_0^* is stable and H_U^* does not exist, or in other words is biologically not relevant, whereas for $r > 0$, H_0^* is unstable and H_U^* is a stable equilibrium.

Similarly, the microscopic interactions between phages and bacteria can be captured by additional reaction kinetics equations. More specifically, we consider free living phages, P , that can infect hosts, and assume that infected hosts become passive in the sense that they are no longer able to reproduce or compete for resources with other hosts and perish generally at a faster rate than their uninfected counterparts, $d > d_U$.

Single phages infect uninfected hosts at rate μ_1 , producing singly infected hosts, H_1 , while two phages simultaneously infect an uninfected host cell at rate μ_2 , producing doubly infected host cells, H_2 . Singly infected host cells can be infected again (at rate μ_1) and become doubly infected hosts. We assume that host cells are never infected by more than two phages to ensure that the dynamics remain analytically tractable. This assumption is supported by empirical evidence that infections are limited to few φ_6 phages per cell (Turner et al., 1999); besides, very high phage densities are required for simultaneous triple infections to significantly affect the dynamics.

After infection, phages replicate inside the host cell. Once the phage particle count inside the host cell has

reached a threshold, say λ on average, the host lyses and releases phages back into the environment. We assume that lysing occurs once host resources are exhausted, and that the replication rate of phages is high, so the lysis time and final count of phage particles released is independent of whether one or two phages infected the host cell. Finally, we also assume that the phage densities are sufficiently higher than bacteria such that impacts of infection events on the phage pool can be neglected, see appendix S3. The rate at which infected hosts die is d , while phages degrade at the rate $d\kappa$. Hence, for $\kappa > 1$ phages are shorter lived than infected hosts, while for $\kappa < 1$ phages outlive hosts.

The corresponding reaction kinetics equations are:

(eq:phageInfection)



Note that single infection events happen at rate $\mu_1 P$ while double infections happen at rate $\mu_2 P^2$. Consequently it seems natural that each infection in a double infection event occurs at rate $\mu_1 P$, and hence $\mu_2 P^2 = (\mu_1 P)^2$ such that $\mu_2 = \mu_1^2$. This allows us to eliminate one parameter by setting $\mu_1 = \mu$ and $\mu_2 = \mu^2$, but keeping the rates separate provides further insights into interesting dynamical details.

Following the mass-action principle, Eqs. (S1), (S3) yield the following system of dynamical equations for the densities of uninfected hosts, H_U , single infected hosts H_1 , double infected hosts H_2 , and free phage particles, P :

(eq:intermediateEqns)

$$\dot{H}_U = r H_U - \xi H_U^2 - \mu_1 H_U P - \mu_2 H_U P^2 \quad [\text{S4a}]$$

$$\dot{H}_1 = \mu_1 H_U P - \mu_1 H_1 P - d H_1 \quad [\text{S4b}]$$

$$\dot{H}_2 = \mu_1 H_1 P + \mu_2 H_U P^2 - d H_2 \quad [\text{S4c}]$$

$$\dot{P} = d \lambda (H_1 + H_2) - d \kappa P. \quad [\text{S4d}]$$

Finally, and again for analytical tractability, we define $H_I = H_1 + H_2$ and simplify our equations into the following, final system of dynamical equations for the densities of uninfected hosts, H_U , infected hosts H_I and

free phage particles, P :

{eq:appModelEqs}

$$\dot{H}_U = r H_U - \xi H_U^2 - \mu_1 H_U P - \mu_2 H_U P^2 \quad [\text{S5a}] \quad \{\text{eq:appdotHu}\}$$

$$\dot{H}_I = \mu_1 H_U P + \mu_2 H_U P^2 - d H_I \quad [\text{S5b}] \quad \{\text{eq:appdotHi}\}$$

$$\dot{P} = d \lambda H_I - d \kappa P. \quad [\text{S5c}] \quad \{\text{eq:appdotP}\}$$

Note that the term related to the conversion of single infected to double infected hosts was lost in the grouping to produce equations Eqs. (S5a), (S5c). See appendix S2 for an alternative derivation of our model that considers sequential infections only and assumes that a second infection can only occur in a small time window after the first infection.

S2 Double infections through susceptible time window

{app:susWin}

As an alternate derivation of our dynamical system, we can assume that only single infections occur (at rate μ_1) but that a second, sequential infection can occur. However, we assume that singly infected hosts remain susceptible only for a short period, which is too brief for lysing to occur. This results in the following system of differential equations with H_{1s} denoting singly infected but susceptible hosts:

{eq:SW_firstmodelEqs}

$$\dot{H}_U = r H_U - \xi H_U^2 - \mu_1 H_U P \quad [\text{S6a}]$$

$$\dot{H}_{1s} = \mu_1 H_U P - \mu_1 H_{1s} P - \eta H_{1s} \quad [\text{S6b}] \quad \{\text{eq:1s}\}$$

$$\dot{H}_1 = \eta H_{1s} - d H_1 \quad [\text{S6c}]$$

$$\dot{H}_2 = \mu_1 H_{1s} P - d H_2 \quad [\text{S6d}]$$

$$\dot{P} = d \lambda (H_1 + H_2) - d \kappa P. \quad [\text{S6e}]$$

We assume a small susceptible time window, $\eta \gg \mu_1 P$. Further, $H_U \gg H_{1s}$ because $H_{1s} \ll H_I = H_1 + H_2$ and $H_I < H_U$ (recall our assumption that infected hosts die faster than uninfected hosts). Overall, hosts pass quickly through the susceptible state, and thus the equilibration of susceptible infected hosts is reasonable. With the assumption $\eta \gg \mu_1 P$ we obtain at equilibrium $H_{1s}^* \approx \frac{\mu_1 H_U P}{\eta}$. This allows to eliminate Eq. (S6b) and insert the equilibrium to obtain:

{eq:SW_finalmodelEqs}

$$\dot{H}_U = r H_U - \xi H_U^2 - \mu_1 H_U P - \mu_2 H_U P^2 \quad [S7a]$$

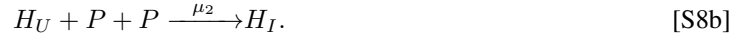
$$\dot{H}_I = \mu_1 H_U P + \frac{\mu_2}{\eta} H_U P^2 - d H_I \quad [S7b]$$

$$\dot{P} = d \lambda H_I - d \kappa P. \quad [S7c]$$

with $H_I = H_1 + H_2$, which is equivalent to eq. 5 with $\mu_2 = \mu_1^2/\eta$.

S3 Infection and phage density

Keeping phage densities constant in our model is conducive to analytical tractability and does not impact the qualitative dynamics. If infections deplete phage densities, then the reaction kinetic equations describing interactions between uninfected hosts and phages are



The resulting system of dynamical equations is identical to Eq. (1) except the equation for \dot{P} , which becomes:

$$\dot{P} = d \lambda H_I - \mu_1 H_U P - \mu_2 H_U P^2 - d \kappa P. \quad [S9]$$

The resulting bifurcation diagram exhibits the same qualitative dynamics as the original model, compare Fig. S1 to Fig. 3 in the main text.

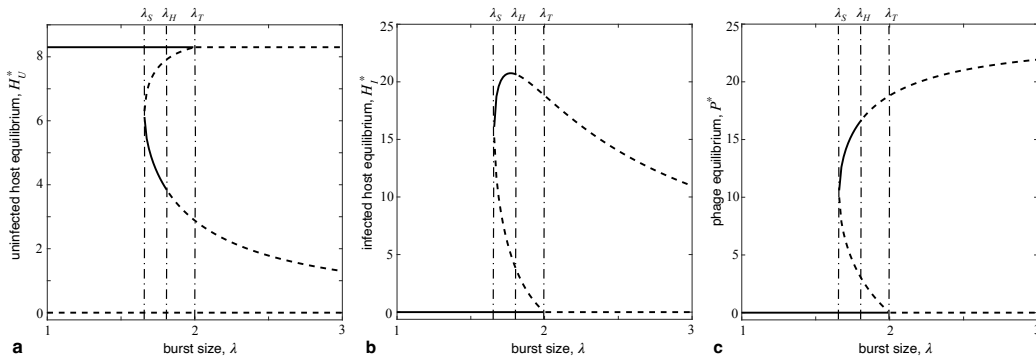


Fig. S1. Bifurcation diagram for Eq. (S9). There are three bifurcation: first a saddle node bifurcation at $\lambda_S \approx 1.66$, next a Hopf bifurcation at $\lambda_H \approx 1.82$, and finally at transcritical bifurcation at $\lambda_T \approx 2.01$. This is the same series of bifurcations seen in the original model, though the exact values of the bifurcations have changed. All parameter values are identical to the manuscript ($r = 8.3, d = 8.3, \kappa = 1, \mu_1 = 0.1, \mu_2 = 0.01, \xi = 0.1$).

We can re-derive R_0 as follows: To calculate the expected lifespan of a phage, or the expected length of time for which a phage has the potential to infect a host cell, we must consider two terms: (i) $\mu_1 H_U P$ and (ii) $d\kappa P$. Thus, when a phage is introduced into an entirely uninfected host cell population with $H_U = r/\xi$, the expected lifespan of a phage is $(\kappa d + \mu_1(r/\xi))^{-1}$. The per capita rate of infection is μ_1 , so a phage introduced into an entirely uninfected host cell population infects $\mu_1(r/\xi)((\kappa d + \mu_1(r/\xi))^{-1})$ cells on average. Thus, initially each phage produces $R_0 = \mu_1 r \lambda / (\mu_1 r + d\kappa \xi)$ new phages, and phages can invade if $\lambda > 1 + (d\kappa \xi / \mu_1 r)$.

S4 Stability analysis

{app:jacobian}

Because hosts undergo logistic growth in the absence of phages, we know the extinction equilibrium E_0 is unstable as long as $r > 0$. The stability of other equilibria requires more work. After noting relationships between dynamical variables at equilibrium, we can write the Jacobian of the dynamical system, Eq. (1) in the main text, as:

$$J = \begin{pmatrix} -\xi H_U & 0 & -2d\frac{\kappa}{\lambda} + \mu_1 H_U \\ r - \xi H_U & -d & 2d\frac{\kappa}{\lambda} - \mu_1 H_U \\ 0 & d\lambda & -d\kappa \end{pmatrix}. \quad [\text{S10}]$$

An equilibrium is stable if the (real parts of) all eigenvalues are negative and unstable if at least one is positive. At the uninfected equilibrium, E_U , the Jacobian is

$$\begin{pmatrix} -r & 0 & \frac{-\mu_1 r}{\xi} \\ 0 & -d & \frac{\mu_1 r}{\xi} \\ 0 & d\lambda & -d\kappa \end{pmatrix} \quad [\text{S11}]$$

with eigenvalues $\{-r, -[d(\kappa + 1) \pm \sqrt{(4rd\lambda\mu_1 + d^2\xi(\kappa - 1)^2)/\xi}]/2\}$, which are all negative for $\lambda < d\kappa\xi/(r\mu_1)$. In order to see this, consider the inequality

$$d(\kappa + 1) > \sqrt{\frac{4rd\lambda\mu_1 + d^2\xi(\kappa - 1)^2}{\xi}}. \quad [\text{S12}] \quad \{\text{eq:negeig}\}$$

Note that both sides are positive. After squaring and rearrangements, we obtain

$$\xi d^2((\kappa + 1)^2 - (\kappa - 1)^2) = \xi d^2 4\kappa > 4rd\lambda\mu_1, \quad [\text{S13}]$$

which yields the above threshold for λ . □

S5 Interior equilibria

{app:interior}

S5.1 Derivation of biologically relevant interior equilibria

{biorelIE}

The number of biologically relevant can be determined analytically based on the discriminant as well as Descartes' rule of signs without having to deal with the unwieldy solutions to cubic equations.

The discriminant of a cubic polynomial of the form $p(x) = Ax^3 + Bx^2 + Cx + D$ is given by

$$\Delta = \frac{4(B^2 - 3AC)^3 - (2B^3 - 9ABC + 27A^2D)^2}{27A^2}. \quad [\text{S14}]$$

For $\Delta > 0$, the polynomial $p(x)$ has three distinct real roots, for $\Delta = 0$, either a triple root or two distinct real roots (one is a double root) and finally for $\Delta < 0$, only one real root remains (plus two imaginary roots, which are of no interest in the present context).

In our case, $A = \lambda^4 \mu_2^2$, $B = 2\kappa \lambda^3 \mu_1 \mu_2$, $C = \kappa^2 \lambda^2 (\mu_1^2 - \mu_2 r)$, and $D = -\kappa^3 \lambda \mu_1 r + d\kappa^4 \xi$, c.f. Eq. (7) in the main text. After simplification, we find that Δ is proportional to a function which is quadratic in λ ,

$$\Delta \propto f(\lambda) := \mu_2 r^2 (\mu_1^2 + 4\mu_2 r) \lambda^2 + 2 d\kappa \mu_1 \xi (2\mu_1^2 \xi + 9\mu_2 r) \lambda - 27 d^2 \kappa^2 \mu_2 \xi^2. \quad [\text{S15}] \quad \text{{eq:deltan}}$$

The function $f(\lambda)$ is an upwards facing parabola with two real roots:

$$\lambda_{\pm} := \frac{d\xi\kappa}{\mu_2 r^2} \frac{-2\mu_1^3 - 9\mu_1 \mu_2 r \pm 2(\mu_1^2 + 3\mu_2 r)^{\frac{3}{2}}}{\mu_1^2 + 4\mu_2 r}. \quad [\text{S16}] \quad \text{{eq:lambdapm}}$$

Clearly, the root λ_- , is always negative and thus not biologically relevant. However, λ_+ turns out to be always positive because $2(\mu_1^2 + 3\mu_2 r)^{3/2} > \mu_1(2\mu_1^2 + 9\mu_2 r) > 0$, which is easy to see after squaring both sides. Thus, whether λ is smaller, equal to or larger than λ_+ determines the sign of Δ and accordingly the number of real roots. Hereafter, we refer to λ_+ as λ_S .

The number of positive roots can then be determined by Descartes' rule of signs, which states that the number of positive roots is equal to the number of sign changes between consecutive, non-zero coefficients or an even number less than that. In Eq. (7) of the main text, A and B are always positive and D is positive for $\lambda < d\kappa\xi/(r\mu_1) =: \lambda_T$. Note that $\lambda_S < \lambda_T$ always holds, see appendix S5.2. The sign of C depends on the growth rate r , which creates two general cases for the number of positive roots:

- (i) $r < \mu_1^2/\mu_2$: for $\lambda < \lambda_T$ no positive root and a single root for $\lambda > \lambda_T$;
- (ii) $r = \mu_1^2/\mu_2$: in this non-generic case $C = 0$ and $\lambda_S = \lambda_T$. Hence, no positive root for $\lambda < \lambda_T$ and still a single root for $\lambda > \lambda_T$;
- (iii) $r > \mu_1^2/\mu_2$: no root for $\lambda < \lambda_S$, two positive roots for $\lambda_S < \lambda < \lambda_T$, and a single root for $\lambda > \lambda_T$.

S5.2 $\lambda_S \leq \lambda_T$

{app:lamSlamT}

In order to show that $\lambda_S \leq \lambda_T$, we need to establish

$$\frac{d\xi \kappa}{\mu_2 r^2} \frac{\mu_1(2\mu_1^2 + 9\mu_2 r) - 2(\mu_1^2 + 3\mu_2 r)^{\frac{3}{2}}}{\mu_1^2 + 4\mu_2 r} \leq \frac{\kappa d\xi}{\mu_1 r} \quad [\text{S17}] \quad \{\text{eq:1S1ess1T}\}$$

which simplifies to

$$\mu_1(\mu_1^2 + 3\mu_2 r)^{\frac{3}{2}} \leq \mu_1^4 + 5r\mu_1^2\mu_2 + 2r^2\mu_2^2. \quad [\text{S18}] \quad \{\text{eq:1s1t}\}$$

Now consider the function $f(r) := \mu_1^4 + 5r\mu_1^2\mu_2 + 2r^2\mu_2^2 - \mu_1(\mu_1^2 + 3\mu_2 r)^{\frac{3}{2}}$, i.e. the difference between the two sides of the inequality Eq. (S18). For $r \geq 0$, $f(r)$ has roots at $r = 0$ and $r = \mu_1^2/\mu_2$. The slope at $r = 0$ is positive and the root at $r = \mu_1^2/\mu_2$ is a local minimum. As a consequence $f(r) \geq 0$ holds for $r > 0$ and hence the inequality Eq. (S18) is always satisfied with equality only for $r = \mu_1^2/\mu_2$ (as well as in the limit $r \rightarrow 0$). \square

S6 H_U^* is positive when H_I^* is positive

{app:boundHI}

From Eq. 7 of the main text we see that H_U^* can be negative if $H_I^* > \kappa(-\mu_1 + \sqrt{\mu_1^2 + 4\mu_2 r})/(2\mu_2\lambda)$. Recall that H_I^* are the roots of the cubic polynomial $f(H_I)$, Eq. 8 in the main text. Here we show that $f(H_I)$ has no roots at or above the threshold, meaning H_I^* is bounded below the threshold, and consequently H_U^* is always positive when H_I^* is positive.

We denote the threshold $\hat{H}_I := \kappa(-\mu_1 + \sqrt{\mu_1^2 + 4\mu_2 r})/(2\mu_2\lambda)$. First note that $f(\hat{H}_I) = d\kappa^4\xi/\lambda > 0$. Therefore \hat{H}_I is not a solution to $f(H_I)$, so $H_I^* \neq \hat{H}_I$. We now show that $f(H_I) > 0$ for $H_I > \hat{H}_I$ and does not admit solutions to $f(H_I) = 0$ for $H_I > \hat{H}_I$.

First, $f'(\hat{H}_I) = \frac{1}{2}\lambda\kappa^2(\mu_1\sqrt{\mu_1^2 + 4\mu_2 r} + \mu_1^2 + 4\mu_2 r) > 0$. Second, the second derivative of $f(H_I)$ is

$$f''(H_I) = 6H_I\lambda^4\mu_2^2 + 4\kappa\lambda^3\mu_1\mu_2,$$

which is positive for $H_I > 0$. Therefore $f'(H_I) > 0$ for $H_I > \hat{H}_I$. In summary, $f(H_I)$ is positive at \hat{H}_I and only increases, and consequently no roots $H_I^* \geq \hat{H}_I$ exist. \square

S7 Single infections dominate at E_I for $r < 2\mu_1^2/\mu_2$

{app:VstarAnalysis}

At the interior equilibrium, E_I , single infections dominate for sufficiently small r . More specifically, single infections dominate when $P^* < \mu_1/\mu_2$. Using Eq. (2) this condition becomes $H_I^* < \kappa\mu_1/(\lambda\mu_2)$. After setting

$x = H_I^* \lambda \mu_2 / (\kappa \mu_1)$ in Eq. (4) of the main text, some algebra yields

$$\frac{d\kappa\xi}{\lambda\mu_1} + (x+1) \left(\frac{\mu_1^2}{\mu_2} x(x+1) - r \right) = 0, \quad [\text{S19}] \quad (\text{eq:CeEq})$$

which at the threshold, $x = 1$, simplifies to

$$\frac{d\kappa\xi}{2\lambda\mu_1} + 2\frac{\mu_1^2}{\mu_2} - r = 0. \quad [\text{S20}] \quad (\text{eq:Ce1})$$

Thus, the left hand side (LHS) of Eq. (S20) is strictly positive for $r < 2\mu_1^2/\mu_2 + d\kappa\xi/(2\lambda\mu_1)$, which means that no solution exists to Eq. (S19) and hence $P^* = \mu_1/\mu_2$ never holds. Note that the only negative term of Eq. (S19) involves r and hence the LHS is minimized when r attains its maximum value. Instead of the maximum we use a smaller $r = 2\mu_1^2/\mu_2$ to simplify the analysis and Eq. (S19) becomes

$$\frac{d\kappa\xi}{\lambda\mu_1} + \frac{\mu_1^2}{\mu_2} (x^2 - 1)(x + 2) = 0. \quad [\text{S21}] \quad (\text{eq:CeEqigr})$$

No solutions to Eq. (S21) with large x exist because the LHS is strictly positive. However, for $x < 1$ one term becomes negative. For any solution to Eq. (S21), $x < 1$ must hold, and hence $P^* < \mu_1/\mu_2$ holds for $r \leq 2\mu_1^2/\mu_2$. Thus, for all r in our first dynamical regime $r < \mu_1^2/\mu_2$ we know that single infections dominate at E_I . \square

However, for $r > 2\mu_1^2/\mu_2$, solutions with $x = 1$, or equivalently $H_I^* = \kappa\mu_1/(\lambda\mu_2)$, must hold for sufficiently large λ . Solving Eq. (S20) yields the $\hat{\lambda}$ for which $H_I^* = \kappa\mu_1/(\lambda\mu_2)$:

$$\hat{\lambda} = \frac{d\kappa\xi\mu_2}{2\mu_1(\mu_2 r - 2\mu_1^2)}.$$

Interpreting $\hat{\lambda}$ requires closer consideration. When $r > \mu_1^2/\mu_2$ (bi-stability possible), a pair of equilibria branch from a single point at the saddle node bifurcation λ_S . We can find expressions for this point by finding where Eq. (4) has a double root. For our analysis, we need only consider the P component of the double root, which we'll denote $Z = g(r)$, as the location of the double root is dependent on r .

In the following analysis, we assume that $\mu_1 = \mu$ and $\mu_2 = \mu^2$. When $r = 8$, then $Z = 1/\mu$ and is located on the boundary between the regions where single versus double infections dominate. This means that $\hat{\lambda} = \lambda_S$, and the top branch E_{I_U} is always in the region where single infections dominate while the bottom branch E_{I_S} is always in the region where double infections dominate. When $r > 8$, then Z is located in the region where double infections dominate and $\hat{\lambda}$ corresponds to where the bottom branch (E_{I_U}) crosses into the region where

single infections dominate, compare to Fig. 3C. Finally, when $2(\mu_1^2/\mu_2) = 2 < r < 8$, then Z is located in the region where single infections dominate, but the top branch (E_{I_U}) will cross the threshold at $\hat{\lambda}$.

It follows that when $r > 2\mu_1^2/\mu_2$, either double infections always dominate at the stable interior equilibrium E_{I^s} , or else double infections will eventually dominate at that equilibrium for sufficiently large $\lambda > \hat{\lambda}$.

S8 Parameters & comparison to previous results

The model of (Beretta and Kuang, 1998), hereafter B&K, is similar in form to Eq. (1) but considers only single infections. Accordingly, Eq. (1) can be interpreted as a generalized model that encompasses B&K but also reveals interesting dynamical features arising through simultaneous infections. As such, a comparison of results from B&K and Eq. (1) is of interest. This comparison is particularly relevant because B&K use $r > \mu_1^2/\mu_2$, part of the parameter case where Eq. (1) exhibits bi-stability. This indicates that simultaneous double infections impact dynamics for B&K's parameters, an effect that their model cannot account for.

Parameter	Value	Comparison to parameter values in (Beretta and Kuang, 1998)
r	$(r > \mu_1^2/\mu_2) : 8.3$	same order of magnitude as corresponding α
	$(r < \mu_1^2/\mu_2) : 0.7$	one order of magnitude smaller than above
ξ	0.1	differs from equivalent (α/C) by 10^6
μ_1	0.1	differs from equivalent K by 10^7 .
$\mu_2 = \mu_1^2$	0.01	no double infections in B&K
d	8.3	same order of magnitude as corresponding λ
κ	1	viral death rate $d\kappa$ on same order of magnitude as corresponding parameter μ
λ	bifurcation parameter	corresponds to bifurcation parameter b

Table 1

Column 1 of Table 1 lists our parameter values while column 2 compares our parameters to those from B&K. Most analogous parameters are on the same order of magnitude, but two parameters are not closely aligned: ξ differs from its equivalent (α/C) by 10^6 while μ_1 differs from its equivalent K by 10^7 . However, these differences can be understood as a rescaling of density, see appendix S8.1 for more details.

As such, we can compare and contrast our results for $r > \mu_1^2/\mu_2$ to those of B&K. There are similarities between the results: for small λ the uninfected equilibrium is the only biologically relevant equilibrium, for $R_0 > 1$ phage can invade, and both models exhibit limit cycles for sufficiently high λ . These similarities

support the interpretation of Eq. (1) as a generalization of B&K.

However, there is a crucial difference: Eq. (1) admits a region of bi-stability where phages introduced through a sufficiently large shock can co-exist with hosts, either at a stable internal equilibrium or through the oscillations of a limit cycle, though $R_0 < 1$. In other words, phages can persist even though they cannot invade. Indeed, in the regime of limit cycles small shocks in phage density are sufficient to establish stable co-existence despite $R_0 < 1$. In summary, accounting for simultaneous double infections predicts that there is a range of λ where, though $R_0 < 1$, hosts are vulnerable to sustained infection after shocks in phage density.

S8.1 Rescaling density

The large differences between our ξ and μ and the analogous parameters (α/C) and K in B&K can be understood as a rescaling of density. To see this, consider respective rescaled densities of uninfected hosts, infected hosts, and phages: $X = (1/c_1)H_U$, $Y = (1/c_2)H_I$, $Z = (1/c_3)P$. Assuming $\mu_1 = \mu$, $\mu_2 = \mu_1^2$, and that $c_1 = c_2$, or that uninfected and infected hosts are rescaled in the same way, Eq. (1) becomes

$$\dot{X} = r X - \hat{\xi} X^2 - \hat{\mu} X Z - \hat{\mu}^2 X Z^2 \quad [\text{S22a}]$$

$$\dot{Y} = \hat{\mu} X Z + \hat{\mu}^2 X Z^2 - d Y \quad [\text{S22b}]$$

$$\dot{Z} = d \hat{\lambda} Y - d \kappa Z \quad [\text{S22c}]$$

where $\hat{\xi} = c_1 \xi$, $\hat{\mu} = c_3 \mu$, and $\hat{\lambda} = (c_2/c_3)\lambda$.

In interpretation, Eq. (S22) indicates that rescaling density results in a rescaling of three parameters: ξ , μ , and λ . This is consistent with a comparison between our parameters and results and those of B&K: all analogous parameters are on the same order of magnitude with the exception of ξ and μ , and bifurcation values have shifted, consistent with a rescaling of the bifurcation parameter λ .

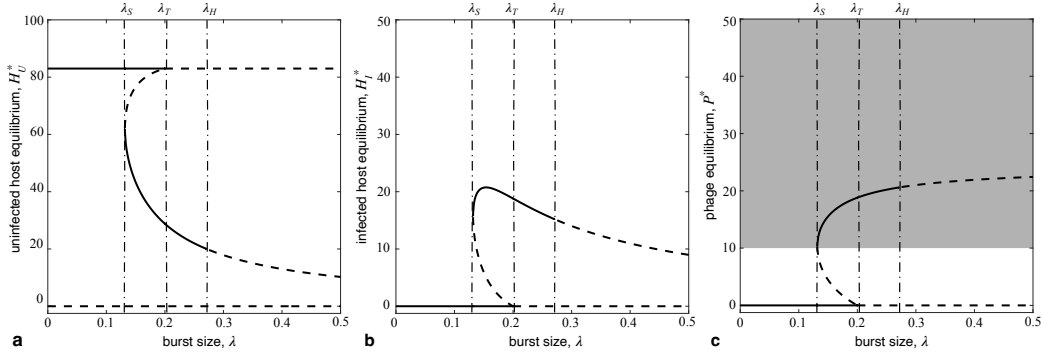


Fig. S2. Bifurcation diagram for the dynamics in Eq. (4) of the main text with $\kappa < 1$ and $r > \mu_1^2/\mu_2$ as a function of the burst size λ . Each panel depicts one component of the stable (solid lines) and unstable (dashed lines) equilibria, $E_i = (H_U^*, H_I^*, P^*)$: **a** uninfected hosts, H_U^* , **b** infected hosts, H_I^* , and **c** phage densities, P^* , where the shaded area marks densities for which double infections dominate. The trivial equilibrium, E_0 , is always unstable and the uninfected equilibrium E_U is stable for small λ . There are three bifurcations (dash-dotted vertical lines): a saddle node bifurcation at $\lambda_S = 0.1317$ (c.f. λ_- in Eq. (S16)) where a pair (stable, E_{I^s} and unstable, E_{I^u}) of interior equilibria appear; a transcritical bifurcation at $\lambda_T = 0.2000$ where the (originally) unstable interior equilibrium, E_{I^u} , disappears and E_U loses stability; and finally Hopf-bifurcation at $\lambda_H \approx 0.2707$ where E_{I^s} loses its stability. This results in four dynamical regimes: for $\lambda < \lambda_S$ the uninfected equilibrium, E_U , is stable and a global attractor; for $\lambda_S < \lambda < \lambda_T$ the dynamics are bi-stable with attractors E_U and E_{I^s} ; for $\lambda_T < \lambda < \lambda_H$ the infected equilibrium E_{I^s} is stable and a global attractor; finally, for $\lambda > \lambda_H$ no stable equilibria exist but there is a stable limit cycle, see Fig. S3 d, h. Parameters: $r = 8.3$, $\xi = 0.1$, $\mu_1 = 0.1$, $\mu_2 = 0.01$, $d = 8.3$, $\kappa = 0.2$ (same as in Fig. 3 except κ).

{fig:k11rg1}

S9 Longevity of hosts versus phages, κ

{app:kappa}

For $\kappa < 1$ phages are longer lived and their densities in the environment are higher. This increases infections such that lower burst sizes λ are required to trigger qualitative changes in dynamics. The saddle node bifurcation λ_S , and transcritical bifurcation λ_T are linear functions of κ and hence maintain their ordering. However, because we have no analytical expression for λ_H , we turn to numerical analysis to determine the impact of κ .

For $r < \mu_1^2/\mu_2$, the ordering of bifurcations remains the same $\lambda_S < \lambda_T < \lambda_H$ regardless of κ and the dynamics remain qualitatively unchanged, see Figs. 1 & 2 in the main text. Similarly, for $r > \mu_1^2/\mu_2$ and $\kappa \geq 1$ the dynamics again remain qualitatively unchanged, see Figs 3 & 4 in the main text, and the ordering of bifurcations remains $\lambda_S < \lambda_H < \lambda_T$. Only for $r > \mu_1^2/\mu_2$ and $\kappa < 1$ the ordering changes to $\lambda_S < \lambda_T < \lambda_H$, see Fig. S2. Most importantly, the interior equilibrium becomes a global attractor for $\lambda_T < \lambda < \lambda_H$, see Fig. S3c, g. This dynamical behavior was seen previously for $r < \mu_1^2/\mu_2$ (see Fig. 1b, e in the main text). In both scenarios, the transcritical bifurcation λ_T occurs before the Hopf bifurcation λ_H .

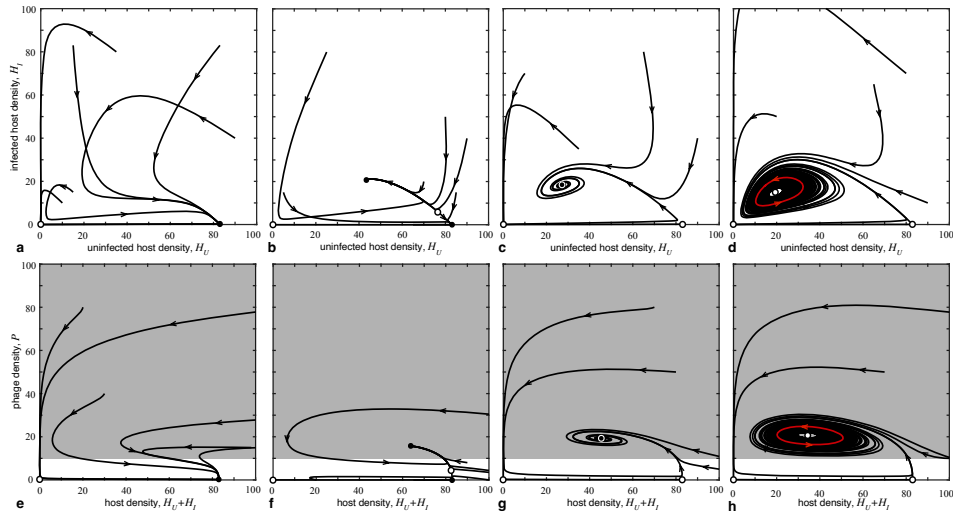


Fig. S3. Projections of the phase space depicting the characteristics of the four dynamical regions for $\kappa < 1$ and $r > \mu_1^2/\mu_2$. The top row shows infected, H_I , versus uninfected, H_U , host densities and the bottom row shows phage densities, P , versus host densities, $H_U + H_I$. Shaded regions on the bottom row mark phage densities for which double infections dominate. Note that trajectories may cross because the panels show projections of a three dimensional phase space. Dots mark stable (filled) and unstable (open) equilibria. Stable limit cycles are shown in red. **a, e** $\lambda = 0.05$: all trajectories converge to E_U and phages go extinct. **b, f** $\lambda = 0.15$: a pair of interior equilibria appear, E_{I^u} and E_{I^s} , and the dynamics become bi-stable with attractors E_U and E_{I^s} . **c, g** $\lambda = 0.21$: the (originally) unstable interior equilibrium E_{I^u} disappears, E_U loses stability, and all trajectories go to the stable global attractor E_{I^s} . **d, h** $\lambda = 0.28$: E_{I^s} loses stability and only a globally stable limit cycle remains. Parameters: same as in Fig. S2.

{fig:ppk11rg1}